Journal of Applied Polymer Science

Structural Development in Ion-Irradiated Poly(ether ether ketone) as Studied by Dielectric Relaxation Spectroscopy

Abdul G. Al Lafi
Department of Chemistry, Atomic Energy Commission, P. O. Box 6091, Damascus, Syrian Arab Republic
Correspondence to: A. G. Al Lafi (E-mail: cscientific@aec.org.sy)

ABSTRACT: Structural alterations to amorphous poly(ether ether ketone) (PEEK) produced by ion irradiation (11.2 MeV H^+ and 25.6 MeV He^{2+} ions) were investigated by dielectric relaxation spectroscopy. The analysis in terms of the Havriliak–Negami (HN) equation and the scaling model showed an increase in the intermolecular correlation with increasing irradiation dose. The dynamic fragility index (m) was estimated from Vogel–Fulcher–Tammann analysis. Ion irradiation not only elevated the glass-transition temperature (T_g) but interestingly decreased m of the PEEK chains around T_g. This was due to increasing polar interaction and better packing efficiency of the irradiated samples compared with those of amorphous PEEK. The average size of the cooperative rearranging region decreased in line with decreasing m and indicated an increase in the rigid amorphous phase fraction after irradiation. The analysis of the direct-current conductivity confirmed that there was a strong coupling between the macroscopic ion transport and concerted segmental motion. © 2013 Wiley Periodicals, Inc. J. Appl. Polym. Sci. **2013**, *000*, 39929.

KEYWORDS: crosslinking; dielectric properties; irradiation

Received 13 June 2013; accepted 4 September 2013
DOI: 10.1002/app.39929

INTRODUCTION

The irradiation of polymers by γ rays, electron beams, or ions initiates a complex series of chemical reactions but, most importantly, crosslinking and chain scission reactions. If irradiation is carried out in the presence of oxygen, peroxy radicals are produced, which readily undergo further reactions; this leads to the functionalization of the irradiated polymer with, for instance, carbonyl and hydroxyl groups.[1]

Poly(ether ether ketone) (PEEK) is an aromatic, high-performance engineering polymer that has an excellent combination of desirable properties for many applications, such as structural materials for aerospace applications and nuclear reactors[2] and in fuel cells as polymer electrolyte membranes.[3]

The structural modification of PEEK by ion irradiation has been accessed qualitatively and quantitatively with a variety of physical, thermal, and mechanical analytical techniques.[2,4–6] It has been shown that crosslinking dominates over other irradiation-initiated reactions. Recently,[7] the dielectric properties of ion-irradiated PEEK were reported with a focus on the regions of low-temperature β and glass α relaxations. Analysis of the β relaxation confirmed that polar groups were attached to the phenyl rings by ion irradiation. On the other hand, analysis of the α relaxation by the Kohlrausch–Williams–Watts function and the coupling model revealed that there was an increase in the interchain coupling between the relaxing units; this was caused by the additional constraints introduced by crosslinking. However, there are many unknown matters regarding the effects of ion irradiation on the dielectrical properties of PEEK.

In this study, the dielectric dispersion curves of ion-irradiated PEEK samples (11.2 MeV H^+ and 25.6 MeV He^{2+} ions) were fitted to the well-known Havriliak–Negami (HN) equation, and the results were associated with the molecular motion in polymers by the use of the scaling model. In addition, the Vogel–Fulcher–Tammann (VFT) function was applied to estimate the dynamic fragility index (m) and other related properties, such as the size of a cooperative rearranging region (CRR) of the irradiated samples. The effect of ion irradiation was also examined in terms of the high-temperature direct-current conductivity (σ_{dc}) of PEEK. An attempt was made to correlate these properties with the irradiation yield.

Such a study is important to help determine significant experimental and theoretical efforts to understand how the chemical structure influences various dynamic processes in polymers.[8–28] It is also important because changes induced by ion irradiation can influence the material applications and its performance in the final product. For example, an increase in the electrical conductivity in power cables will increase losses and lead to heating and other effects.[29] Also, this will result in power losses when PEEK is applied as structural materials in the field of fuel cells.[30]

Table I. Irradiation Setup and Dose Evaluation for H^+ and He^{2+} Ions

Irradiation ions	Total charge ($\times 10^{-4}$ C)	Fluence (C/m^2)[b]	Ions per unit area ($\times 10^{18}$ m^{-2})	Average track spacing ($\times 10^{-10}$ m)	Dose (MGy)[a]
H^+	96.3	9.4	58.65	1.40	37.9
He^{2+}	34.8	3.4	21.20	2.33	42.9

[a] The irradiated area was the same for all samples at 10.24 cm^2.
[b] At the first layer.

EXPERIMENTAL

Amorphous PEEK was obtained from Goodfellow, Ltd. (United Kingdom), as a 100 μm thick film with a density of 1260 kg/m^3. Irradiation with ions was carried out with the University of Birmingham's Scanditronix MC40 Cyclotron operating at 12.5 MeV for protons (H^+) and at 33 MeV for helium ions (He^{2+}). The full irradiation setups were discussed in a previous article.[7] These are summarized in Table I.

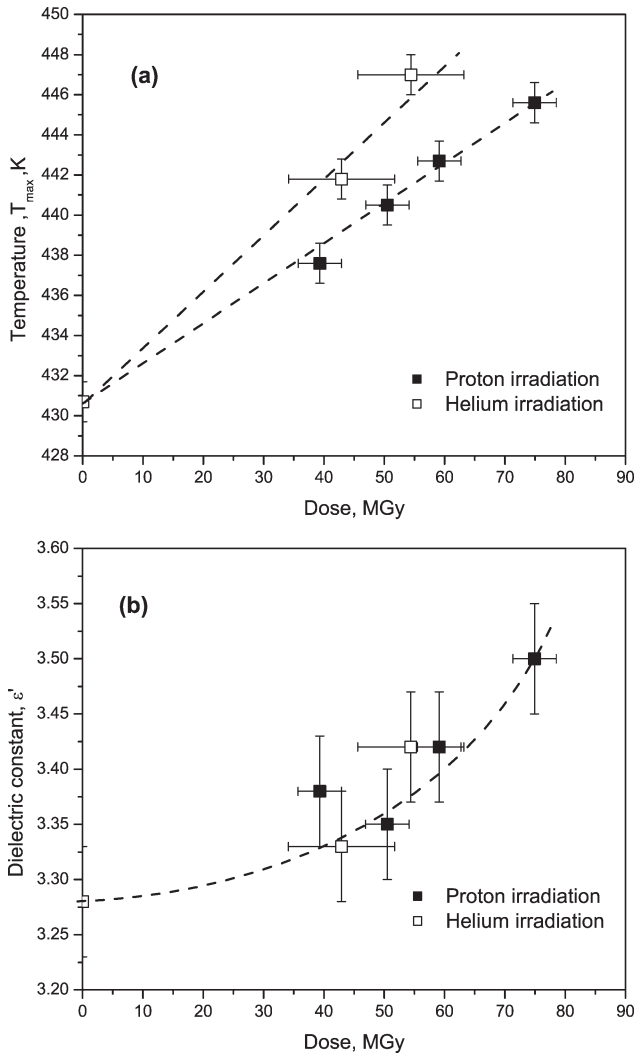

Figure 1. (a) T_{max} at 1 kHz and (b) relative dielectric constant at 323 K and 1 kHz for PEEK samples as a function of the exposure dose. The heating rate was 2 K/min.

The dielectric properties were measured with a dielectric thermal analyzer (Polymer Laboratories, Ltd.) and was operated at a fixed voltage of 1.0 V with a set of frequencies in the range of 50–10^5 Hz. Step isothermal experiments were carried out for the PEEK samples through measurement of both the dielectric loss and dielectric constant at 20 frequencies in the temperature range from 393 to 513 K in steps of 2 or 5 K with a soak time of 10 min between each step. This temperature range allowed the region of glass relaxation to be investigated and minimized the contribution of other relaxation processes, such as crystallization and thermal conductivity. To ensure good electrical contact between the electrodes and the sample, the polymer films

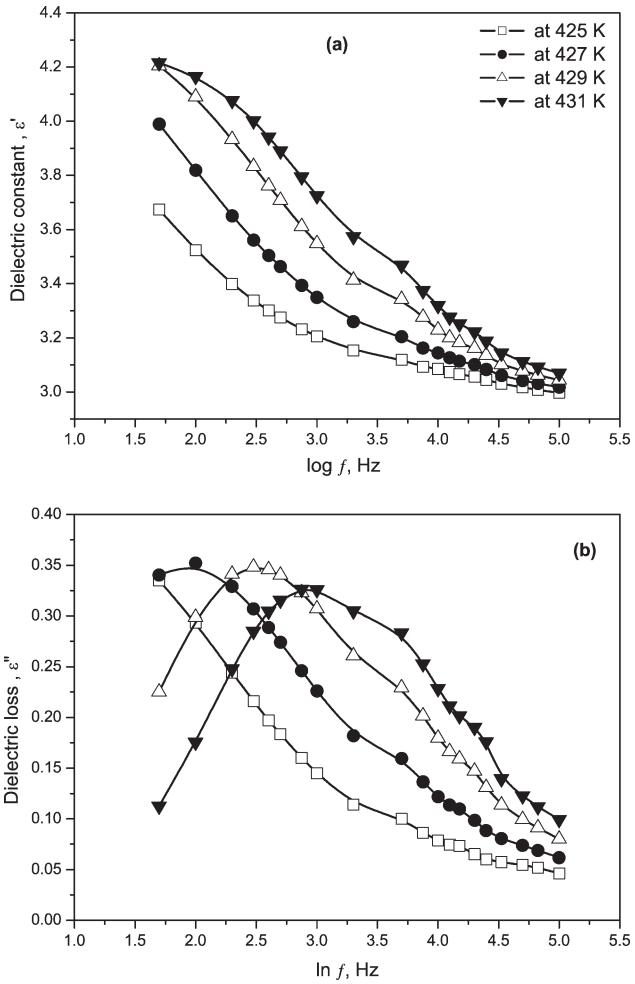

Figure 2. (a) Dielectric constant and (b) dielectric loss as a function of the logarithm of the frequency for amorphous PEEK.

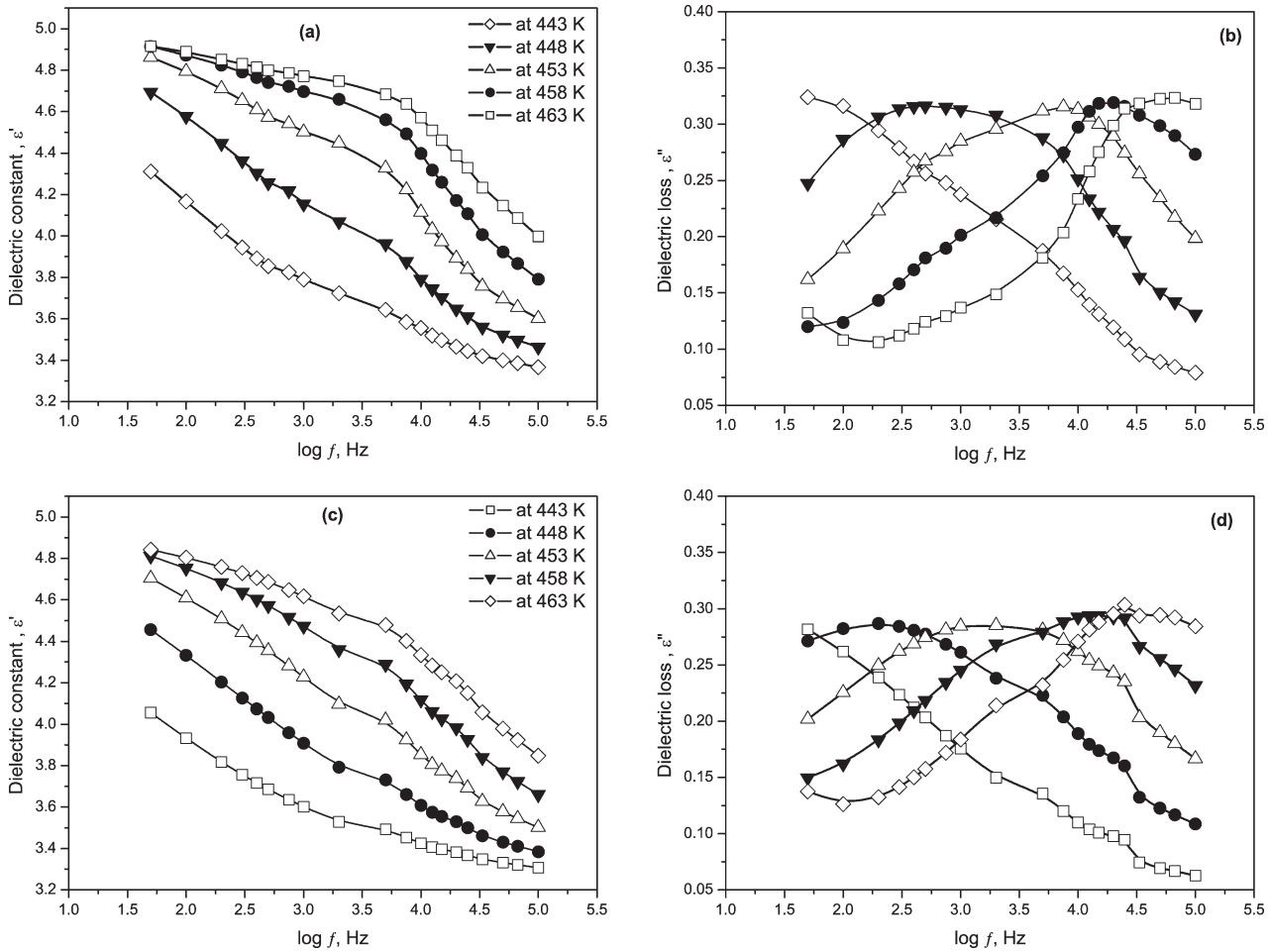

Figure 3. (a,c) Dielectric dispersion curves (ε' vs log f) and (b,d) dielectric loss curves (ε'' vs log f) for (a,b) proton-irradiated PEEK with 74.9 MGy and (c,d) helium-irradiated PEEK with 54.4 MGy in the region of glass relaxation. ε'' is the dielectric loss.

were sputter-coated with a thin layer of gold with a Polaron E5000 sputter-coating unit. The data were fitted to the HN equation with Plus V5.44 software supplied by Rheometric Scientific (United Kingdom). Fitting was also carried out with graphical methods described elsewhere.[31]

RESULTS AND DISCUSSION

General Irradiation Effects

Ion irradiation affected the dielectric properties of amorphous PEEK in two simultaneous reactions: crosslinking and oxidation via chain scission. Evidence of these two effects is depicted in Figure 1, which shows the analysis of the temperature-dependent dielectric properties of the PEEK samples. As shown in Figure 1(a), the temperature corresponding to a maximum in the dielectric loss (T_{max}) increased with the irradiation dose, and this increase was dependent on the ion used. This was in agreement with the dielectric and calorimetric results reported earlier[4,5,7] and indicated that ion irradiation promoted crosslinking in PEEK.

As shown in Figure 1(b), the relative dielectric constant increased with increasing exposure dose, and this increase was in agreement with the literature studies of electron beam effects on PEEK.[32,33] It was reported that the C—C strength decreased and the C—O and C═O strengths increased with the electron beam irradiation of PEEK.[34] In addition, the affinity of PEEK to the sulfonation reaction was reported to improve on ion irradiation.[35] These suggest that irradiation disintegrates molecules and increases the number of dipoles so that the irradiated specimens produce a larger dielectric constant, ε'.

The relaxation maps of the amorphous PEEK are shown in Figure 2(a,b) for all of the frequencies studied and in the range of temperatures that spanned the region of α relaxation but stopped before crystallization proceeded. As expected, the α relaxation manifested itself as a maximum in the dielectric loss and as a step in the dielectric constant. As the temperature increased, the frequency of maximum loss and the dielectric constant shifted toward higher values. In a comparison of the dielectric constant results, the measured value of amorphous PEEK at 431 K and 10 kHz was 3.4 ± 0.1; this was consistent with the reported value at the same conditions, that is, 3.6 ± 0.1.[36]

The relaxation maps of the ion-irradiated PEEK are shown in Figure 3(a–d) for all of the frequencies studied and in the

region of α relaxation. Similar to amorphous PEEK, as the temperature increased, the frequency of maximum loss and the dielectric constant shifted toward higher values. They also shifted toward higher values with increasing irradiation dose.

HN Equation and the Scaling Model

In analyzing the dielectric loss and dispersion data in the frequency domain, the HN equation[8,31] was used:

$$\varepsilon^* = \varepsilon_\infty + \frac{\varepsilon_0 - \varepsilon_\infty}{\left[1+(iw\tau)^{\beta_{HN}}\right]^{\alpha_{HN}}} \quad (1)$$

where ε^*, ε_0 and ε_∞ are the complex dielectric constant, the low and the high frequency limiting values of the dielectric constant respectively. w is the angular frequency ($w = 2\pi f$) and i is an imaginary number, $0 < \beta_{HN} \leq$ and $0\ \alpha_{HN} \leq 1$, and τ is the relaxation time. The parameters β_{HN} and α_{HN} represent the breadth and skewness of the distribution of τ, respectively. When we plotted the dielectric loss against the dielectric constant for the amorphous and ion-irradiated PEEK samples [see Figure 4(a–c)], skewed semicircular arcs were obtained. Good agreements were obtained between the experimental and theoretical data, which were calculated with the HN model for each sample. This indicated that this routine could be used to describe the dielectric response in this region. Subsequently, α_{HN} and β_{HN} were determined from eq. (1) for PEEK and irradiated PEEK as a function of the irradiation dose and temperature. The results of this analysis are listed in Table II. In comparison, the results for amorphous PEEK were in agreement with other reported literature values.[37]

According to Schlosser and Schönhals,[9,38] two scaling parameters, m and n, were required to relate the molecular motion of the polymer to the HN parameters.[39] They suggest that the mobility of the polymer chain segments at the glass-transition temperature (T_g) was controlled by both intramolecular and intermolecular interactions. m describes the dielectric response in the low-frequency region (i.e., $w\tau \ll 1$) and is related to the intermolecular correlation between the chains and the segments. n describes the dielectric response at high frequency (i.e., $w\tau \gg 1$) and is related to the local chain dynamics. These parameters are correlated with the HN parameters such that $n = \alpha_{HN}\beta_{HN}$ and $m = \beta_{HN}$.

Taking into account the change in T_g due to an increased proportion of units crosslinked with increased ion irradiation dose and normalizing for this difference allows one to define a normalized temperature (T_N) as $T_N = T_g + 15$. Figure 5(a) shows the dependence of both m and n on the crosslinking density at T_N. As shown, n was nearly independent of the crosslinking density; this suggested that the local motions in amorphous PEEK were unaffected by ion irradiation. m, on the other hand, decreased from 0.8 to 0.3 with increasing irradiation dose. According to the scaling model, the decrease in m was explained as due to the increase in the intermolecular correlation. These results are in agreement with previous investigations in networks based on styrene–butyl acrylate divinyl benzene with a moderate degree of crosslinking in which n was not affected.[11] The results were also consistent with other studies on the effects of crosslinking on the dynamics of the polymers.[12,40] Moreover, Figure 5(b) provides evidence of the well-known linear energy transfer (LET) effect such that the helium ions were more effective in crosslinking PEEK than protons at similar doses.[5]

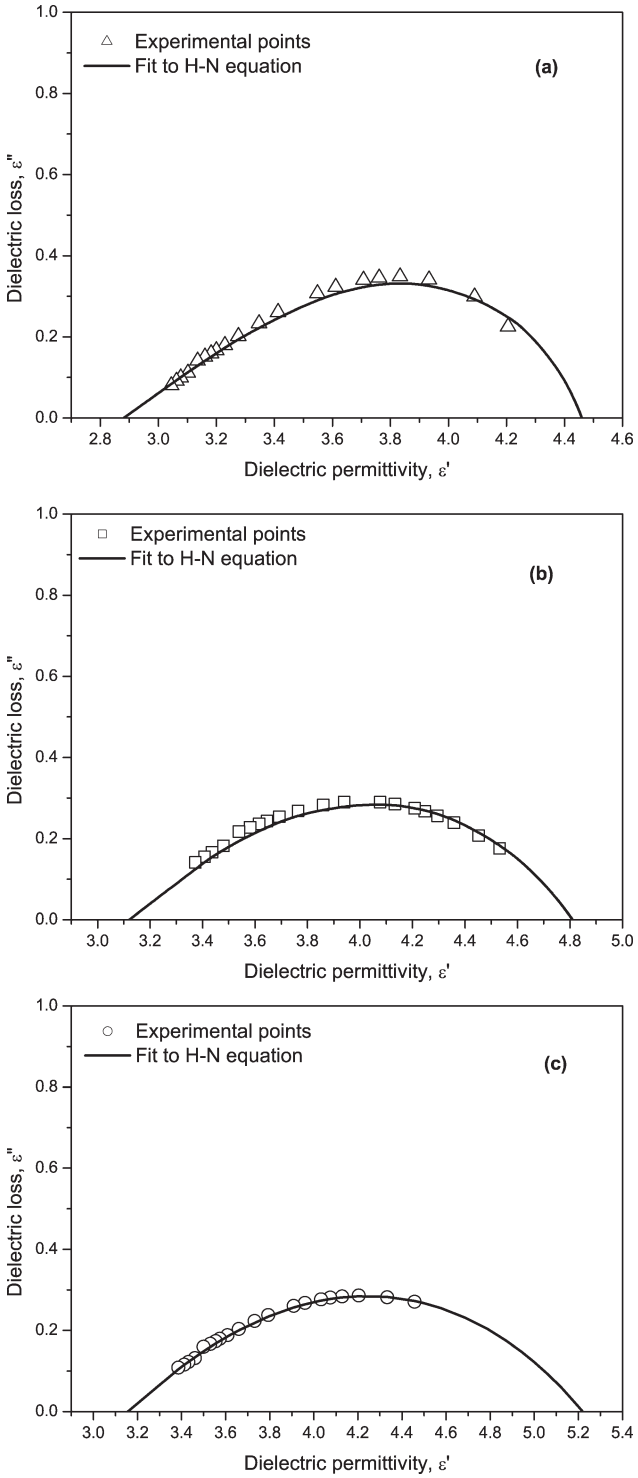

Figure 4. Best fit of the HN relationship to the dielectric loss of (a) amorphous PEEK at 429 K, (b) 59.1 MGy proton-irradiated PEEK at 448 K, and (c) 54.4 MGy helium ion-irradiated PEEK at 448 K.

Table II. Havrilak–Negami Best Fit Parameters for the Amorphous and Ion-Irradiated PEEK

Irradiation	Dose (MGy)	Temperature (K)	$\Delta\varepsilon^a$	β_{HN}	α_{HN}	$\tau \times 10^3$ (s)
Amorphous PEEK	0.0	427	1.66	0.60	0.48	6.90
		429	1.58	0.70	0.43	1.67
		431	1.42	0.76	0.41	0.62
Proton (H^+)	39.3	443	1.42	0.77	0.41	5.1
		448	1.43	0.75	0.40	0.82
		453	1.37	0.62	0.38	0.31
	50.5	443	1.32	0.87	0.39	4.20
		448	1.31	0.76	0.40	0.67
		453	1.28	0.66	0.43	0.24
	59.1	443	1.81	0.85	0.42	1.62
		448	1.69	0.67	0.48	0.26
		453	1.65	0.59	0.55	0.10
	74.9	443	2.19	0.91	0.38	5.47
		448	1.92	0.70	0.45	0.72
		453	1.82	0.66	0.51	0.21
Helium (He^{2+})	42.9	443	1.51	0.76	0.39	6.54
		448	1.41	0.67	0.42	0.77
		453	1.32	0.53	0.50	0.16
	54.4	443	2.23	0.83	0.35	25.4
		448	2.06	0.78	0.37	1.92
		453	2.02	0.61	0.40	0.51

[a] The dielectric strength $\Delta\varepsilon$ is temperature dependent and is defined as $\Delta\varepsilon(T) = \varepsilon_O(T) - \varepsilon_\infty(T)$.

Estimation of *m*

To compare the τ–temperature dependences of systems having different T_g values, the τ values were scaled as a function of T_g/T is the measured temperature, where $T_g = T(\tau_\alpha = 100s)$, τ_α is the relaxation time at the glass transation, and the so-called cooperativity plots were obtained.[14] An example of these plots is shown in Figure 6, in which the τ values for all of the samples studied tended to collapse into a single curve when $T = T_g$. This was in agreement with previous experiments and theoretical predictions.[15] It was evident that the τs for the amorphous and ion-irradiated PEEK samples strongly deviated from Arrhenius behavior, which would have corresponded to a straight line in this plot. The strength parameter (D), which could be evaluated from VFT analysis, is a useful parameter for quantifying deviations from Arrhenius law.[41]

To estimate the steepness index, the experimental data were fitted with the well-known VFT equation,[16] which describes the temperature dependence of segmental τ near T_g, such that

$$\tau = \tau_o \exp\left(\frac{B}{T - T_o}\right) \tag{2}$$

where τ_o, B, and T_o are a pre-exponential factor, VFT fit parameter and the Vogel temperature. τ is the relaxation time at temperature T and was calculated from the dispersion curves as $\tau = 1/2\pi f_{max}$, where f_{max} is the frequency corresponding to a maximum in the dielectric loss. To reduce the effect of data fitting to the VFT equation over a limited frequency range, a value of $\log_{10} \tau_o \approx -14$ was assumed according to the literature.[16] It has been shown that this assumption does not affect the quality of the data fit into the VFT equation but reduces the dispersion among the fitting parameters.[12]

The VFT parameters are related to D, m, and the apparent activation energy (E_g) at T_g as follows:

$$D = \frac{\ln 10 \times B}{T_o} \tag{3}$$

$$m = \frac{B/T_g}{\ln 10\left(1 - T_o/T_g\right)^2} \tag{4}$$

$$E_g = \frac{RB}{\left(1 - T_o/T_g\right)^2} \tag{5}$$

where R is the gas constant (8.314J/Kmol)

Because this estimate of m uses all of the measured data via the VFT fit, it is more accurate than a simple measure of the slope at T_g evaluated directly from a few experimental data points in close proximity to $T = T_g$. The error bars of the m values were estimated from the error bars of the VFT fit parameters, and the results are quoted in Table III. The D values were low, with $D < 10$ corresponding to the most fragile glass-forming materials that showed the largest deviations from Arrhenius law.[41] The D value for the amorphous PEEK was about 2, and it was slightly higher than the reported value of 1.5.[14] The difference

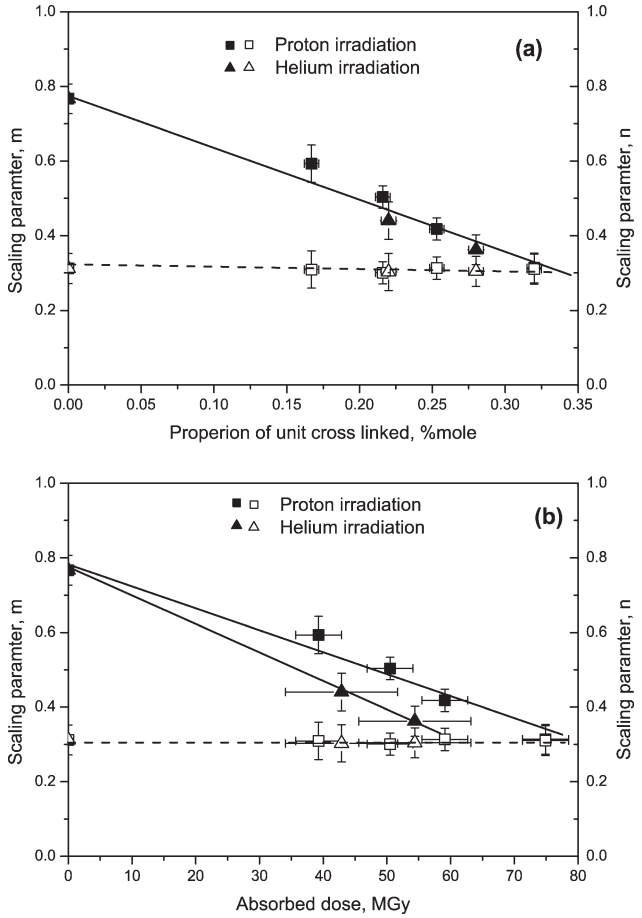

Figure 5. m (solid symbols) and n (open symbols) according to Schönhals and Schlosser plotted at T_N as a function of the (a) crosslinking and (b) absorbed dose. The lines are intended as guides only.

was attributed to the differences in the VFT fitting parameters. In comparison, D of PEEK was lower than that reported for other aromatic polymers, such as poly(ethylene terephthalate) (PET) and polycarbonate from bisphenol A.[13,41] This was attributed to the higher rigidity of the chain structure of PEEK as compared with PET and polycarbonate from bisphenol A.[14] On ion irradiation, D increased to 4.5, and the m and E_g values were reduced compared with those of amorphous PEEK, but the T_g values increased with increasing exposure dose. Moreover, D decreased, and the m and E_g values increased with increasing exposure dose in each set of ions. The D values of helium-irradiated PEEK were larger, and the m and E_g values were smaller than those of the proton-irradiated PEEK. These observations are discussed in the following section.

With some exceptions,[19] the breadth of the relaxation times calculated from the Kohlrausch-Williams-Watts equation (β_{KWW}) of most glass-forming materials is related to their m by an approximate empirical relationship such that $m = (250 \pm 30) - 320\beta_{KWW}$.[41] With $\beta_{KWW} = 0.43$ for amorphous PEEK,[7] one obtained $m = 115 \pm 30$; this was consistent with the estimated value in this study. However, it was reported that β_{WKK} decreased with increasing ion-irradiated dose,[7] and as a results, an increase in m was expected. That was not the case with the irradiated samples. Moreover, according to the Qin and McKenna correlation,[18] m increased with increasing T_g for different classes of polymeric glass formers. This trend, however, breaks down for many systems,[17,19,42] and this study is one example, although the m values and T_g values of the polymers studied in this work showed a broad scattering of the data without a clear trend.

The m values of polymers have been shown to be affected by molecular and dielectric structure parameters.[20,22] Molecular structure parameters are determined by symmetry, rigidity/flexibility, and steric hindrance of the backbone chain and side groups. Dielectric structure parameters are determined by the type and concentration of dielectrically active species (mostly dipoles) and the various specific interactions that can affect the reorientational dynamics of dipoles. The influence and relative contributions that the backbone stiffness and intermolecular interactions have on m and T_g of polymers have been discussed in the literature.[28] It was found that both T_g and m increase with an increase in the backbone stiffness in terms of the bending energy, while the intermolecular interactions remain constant. At the same time, an increase in the intermolecular interactions at a constant bending energy leads to a decrease in m and an increase in T_g. It was also found that more rigid molecules had slower backbone dynamics (higher T_g), but they also had higher packing frustration than flexible molecules. On the other hand, an increase in the intermolecular interactions with a constant backbone rigidity led to an increase in the friction coefficient and to better packing. The former led to a higher T_g, and the latter resulted in a smaller m.[17,28] It seemed that this was the case in the ion-irradiated PEEK samples as it was shown that the intermolecular interaction expressed as $n = 1 - \beta_{KWW}$ increased with ion irradiation.[7] The results were also consistent with those of a recent work[17] on poly(4-methylstyrene) and poly(4-chlorostyrene) pair, where the increase in the intermolecular interactions resulted in a reduction in m and an increase in T_g.

It has been also reported[23] on poly(ethylene oxide) (PEO)-based single-ion-conducting materials that T_g increased whereas m

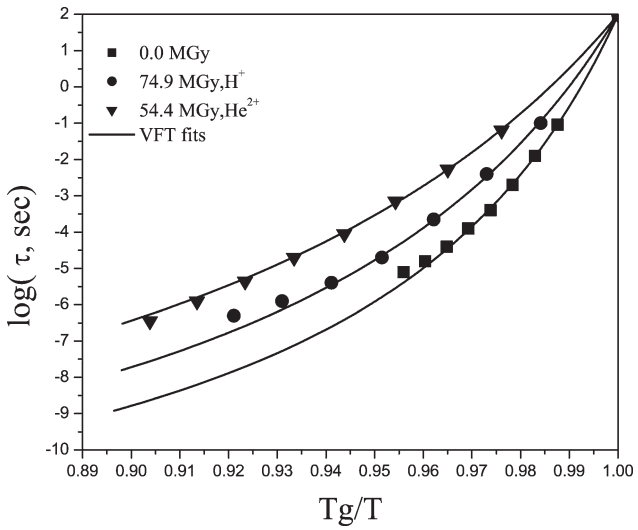

Figure 6. Cooperativity plot of τ as a function of the reduced temperature for amorphous and ion-irradiated PEEK: experimental data (symbols) and their corresponding VFT fits (lines).

Table III. Summary of the VFT Fit Results for the Amorphous and Ion-Irradiated PEEK

Irradiation	Dose (MGy)	T_g^{DSC} (±1.0 K)[a]	$T_g^{(DETA)}$ at 100Hz (±1.0 K)	α Process									
				D ± 0.1	T_o ± 1.0 (K)	E_g ± 0.04 (MJ/mol)	m				σ_{dc}		
							m^b	m^c	$z(T_g)$ ± 1[d]	$z(T_g)$ ± 1[e]	log σ_o ± 0.1 (S/m)	D ± 0.06	
As received	0	418.4	426.8	2.1	395.3	1.26	155 ± 5	280 ± 10	18	18	−5.6	1.7	
Proton (H^+)	39.3 ± 3.6	421.6	432.3	3.3	393.0	1.32	159 ± 5	317 ± 5	15	20	−4.8	2.3	
	50.5 ± 3.6	423.7	435.5	3.3	394.4	1.21	145 ± 4	277 ± 8	15	17	−5.0	2.1	
	59.1 ± 3.6	424.1	437.1	3.2	392.7	1.01	121 ± 5	235 ± 9	14	15	−4.6	2.2	
	74.9 ± 3.6	425.6	439.1	2.9	400.1	1.20	143 ± 5	324 ± 11	17	20	−4.1	2.2	
Helium (He^{2+})	42.9 ± 8.8	425.1	436.8	4.5	375.2	0.70	84 ± 3	124 ± 4	9	8	−3.6	3.2	
	54.4 ± 8.8	427.7	441.2	4.1	384.9	0.80	95 ± 3	159 ± 5	10	10	−3.3	3.4	

[a] Glass-transition temperature as determined from DSC in the first heating scan.
[b] Calculation based on T_g determined from DETA ($T_g^{(DETA)}$).
[c] Calculation based on T_g determined from DSC.
[d] Calculated from eq. (7).
[e] Calculated from eq. (6).

decreased with increasing ion content. In the case of ionomers, the increase in the ion content indicated an increase in the number of highly polar groups that could act as transient crosslinks and slow down the segmental dynamics. At the same time, the ions improved chain packing and decreased m.[17] This explained why the helium-irradiated PEEK samples had lower m values than the proton-irradiated ones.

It was concluded that both crosslinking and oxidation accompanying ion irradiation had effects on the m and T_g values as they both increased the glass transition, but increasing polarity led to a decrease in m. It seemed that the polarity had a greater effect than the chain stiffness in controlling m in these systems.

Average Size of a CRR

It is well known that the molecular motion in the glassy state has a cooperative nature, and the rearranging movement of one structural unit is only possible if a certain number of neighboring structural units are also moved.[24] The average size of a CRR is of prime importance for the description of the relaxation process. The CRR is defined as a subsystem that upon a sufficient thermal fluctuation, can be rearranged into another configuration independently of its environment.[21,26]

The CRR is represented by the quantity $z(T_g)$, which defines the average number of structural units that relax together to cross from one configuration to another. The quantity $z(T_g)$ is related to the Kauzmann temperature, T_k by the equation:[27]

$$z(T_g) = \frac{T_g}{T_g - T_k} \tag{6}$$

According to the literature,[26] the link between m and the average size of a CRR $z(T_g)$ for the polymeric glass-forming liquids is expressed by the following empirical relationship:

$$z(T_g) \approx m/16 \tag{7}$$

The results in Table III reveal that the values of CRR calculated from eq. (6) or estimated from eq. (7) were similar within experimental errors. In addition, the CRR of the ion-irradiated samples decreased in line with decreasing m. From a structural point of view, the decrease in the CRR size indicated that the amorphous phase quantity was drastically reduced because of the presence of crosslinks in this region. This was in agreement with the results reported on the PET samples having different draw ratios where the decrease in the amorphous phase quantity induced a decrease in the CRR size.[25]

DC Conductivity, σ_{dc}

The author determined the extent of σ_{dc} at a high temperature above T_g by fitting the linear portion of the dielectric loss curves in the low-frequency region using the following relation:[23]

$$\varepsilon''(f) = \frac{\sigma_{dc}}{2\pi f \varepsilon_0} \tag{8}$$

where ε_0 and f are the permittivity of free space (8.85×10^{-12} F/m) and the frequency.

Figure 7 displays the results obtained for different amorphous and ion-irradiated PEEK samples plotted as a function of T_N taken as T/T_g. With increasing ion irradiation dose, the high-temperature σ_{dc} increased, and the curves shifted toward lower

T/T_g values because of the increasing number of attached polar groups. Figure 8 represents the calculated σ_{dc} values for the amorphous and ion-irradiated PEEK at a T_N taken as $T/T_g = 1.18$. Two conclusions could be extracted from this graph; first, there was an increase in the conductivity with increasing ion irradiation dose, and second, the helium ions were more effective in producing structural changes in PEEK because of their higher LET compared to the proton ions.[5]

To obtain more information about the conductivity process, the dependence of σ_{dc} on the temperature were fitted to the VFT equation, such that

$$\sigma_{dc} = \sigma_o \exp\left(\frac{B}{T - T_o}\right) \quad (9)$$

where σ_0 is a pre-exponential factor.

The experimental data were fitted to the VFT function with the same T_o values as listed in Table III. The graphical representations of this routine are depicted in Figure 7(a,b) for proton- and helium-irradiated PEEK, respectively, and the results are quoted in Table III. The VFT analysis showed that the D values were close to that of the α process, increasing with increasing ion irradiation dose. This confirmed that for all of the irradiated samples, there

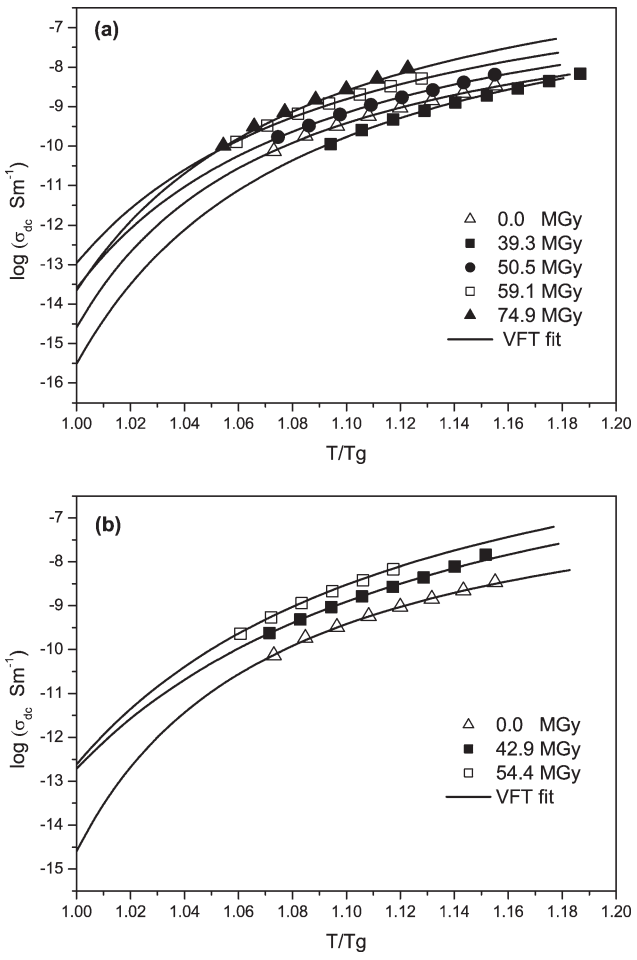

Figure 7. σ_{dc} as a function of T_N (T/T_g) for (a) proton-irradiated and (b) helium-irradiated PEEK. The lines are the fits of the VFT equation with the parameters listed in Table III.

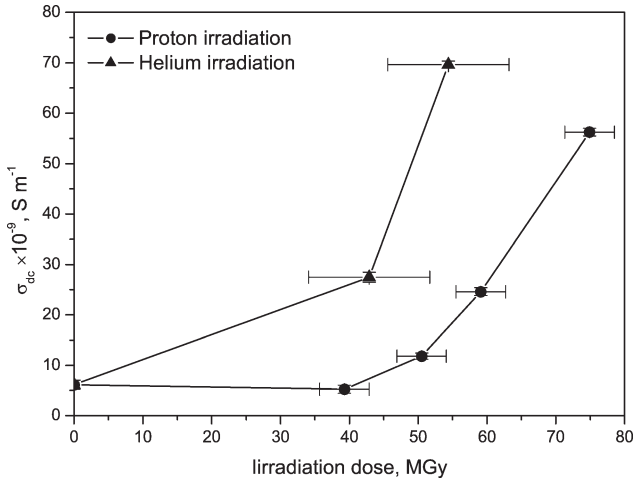

Figure 8. σ_{dc} (calculated at $T/T_g = 1.18$) as a function of the irradiation dose for the proton- and helium-irradiated PEEK.

was a strong coupling between the migration of the ions and the concerted segmental motion of the polymer chains.

CONCLUSIONS

The effect of ion irradiation on the dynamic motion of PEEK was studied by dielectric relaxation spectroscopy. The results were fitted to the HN function and subsequently described in the light of the Schönhals and Schlosser phenomenological model. It was found that increasing crosslinking density did not affect the local motions of PEEK but slowed down the long-range ones. The results of VFT analysis show that ion irradiation not only elevated T_g but interestingly decreased m of the PEEK chains around T_g. This suggested that the polarity had a greater effect than chain stiffness in controlling m in these systems. In addition, the CRR values of the ion-irradiated samples decreased in line with decreasing m. This indicated that the amorphous phase quantity was drastically reduced because of the presence of crosslinks in this region. Finally, there was an increase in the conductivity with increasing ion irradiation dose, and this increase was dependent on the LET of the ions. Although a few polymeric systems have been reported to exhibit similar behavior, the system examined in this study provided an example of complex structural factors that controlled both m and T_g. These factors were produced by the different reactions (oxidation, chain scission, and crosslinking) that occurred simultaneously on ion irradiation and were controlled by the ion used (H^+ and He^{2+}) or the irradiation dose.

ACKNOWLEDGMENTS

The author thanks J. N. Hay for useful discussion and D. J. Parker for allowing the use of irradiation facility and for useful discussion. Thanks are also due to I. Othman, General Director of the Atomic Energy Commission of Syria, and T. Yassine, Head of the Chemistry Department, for their encouragements.

REFERENCES

1. Charlesby, A. Atomic Radiation and Polymers; Pergamon: London, **1960**.

2. Sasuga, T.; Kudoh, H. *Polymer* **2000**, *41*, 185.
3. Chen, J.; Maekawa, Y.; Asano, M.; Yoshida, M. *Polymer* **2007**, *48*, 6002.
4. Al Lafi, A. G.; Hay, J. N.; Parker, D. J. *J. Polym. Sci. Part B: Polym. Phys.* **2008**, *46*, 1094.
5. Al Lafi, A. G.; Hay, J. N.; Parker, D. J. *J. Polym. Sci. Part B: Polym. Phys.* **2008**, *46*, 2212.
6. Mackovà, A.; Havranek, V.; Svorcik, V.; Djourelov, N.; Suzuki, T. *Nucl. Instrum. Meth. Phys. Res. B* **2005**, *240*, 245.
7. Al Lafi, A. G. *Polym. Bull.* **2012**, *68*, 2269.
8. Havriliak, S.; Negami, S. *Polymer* **1967**, *8*, 161.
9. Schlosser, E.; Schönhals, A. *Colloid Polym. Sci.* **1989**, *267*, 963.
10. Fitz, B.; Andjelić, S.; Mijović, J. *Macromolecules* **1997**, *30*, 5227.
11. Glatz-Reichenbach, J. K. W.; Sorriero, L. J.; Fitzgerald, J. *J. Macromolecules* **1994**, *27*, 1338.
12. Kramarenko, V. Y.; Ezquerra, T. A.; Šics, I.; Baltá-Calleja, F. J.; Privalko, V. P. *J. Chem. Phys.* **2000**, *113*, 447.
13. Ngai, K. L.; Roland, C. M. *Macromolecules* **1993**, *26*, 6824.
14. Nogales, A.; Ezquerra, T. A.; Batallán, F.; Frick, B.; López-Cabarcos, E.; Baltá-Calleja, F. *J. Macromolecules* **1999**, *32*, 2301.
15. Ngai, K. L.; Roland, C. M. *Macromolecules* **1993**, *26*, 2688.
16. Angell, C. A. *Polymer* **1997**, *38*, 6261.
17. Agapov, A. L.; Wang, Y.; Kunal, K.; Robertson, C. G.; Sokolov, A. P. *Macromolecules* **2012**, *45*, 8430.
18. Qin, Q.; McKenna, G. B. *J. Non-Cryst. Solids.* **2006**, *352*, 2977.
19. Roland, C. M.; Paluch, M.; Rzoska, S. J. *J. Chem. Phys.* **2003**, *119*, 12439.
20. Kunal, K.; Robertson, C. G.; Pawlus, S.; Hahn, S. F.; Sokolov, A. P. *Macromolecules* **2008**, *41*, 7232.
21. Adam, G.; Gibbs, J. H. *J. Chem. Phys.* **1965**, *43*, 139.
22. Dalle-Ferrier, C.; Niss, K.; Sokolov, A. P.; Frick, B.; Serrano, J.; Alba-Simionesco, C. *Macromolecules* **2010**, *43*, 8977.
23. Fragiadakis, D.; Dou, S.; Colby, R. H.; Runt, J. *J. Chem. Phys.* **2009**, *130*, 064907.
24. Glarum, S. H. *J. Chem. Phys.* **1960**, *33*, 639.
25. Saiter, A.; Dargent, E.; Saiter, J. M.; Grenet, J. *J. Non-Cryst. Solids* **2008**, *354*, 345.
26. Saiter, A.; Saiter, J. M.; Grenet, J. *Eur. Polym. J.* **2006**, *42*, 213.
27. Solunov, C. A. *Eur. Polym. J.* **1999**, *35*, 1543.
28. Stukalin, E. B.; Douglas, J. F.; Freed, K. F. *J. Chem. Phys.* **2009**, *131*, 114905.
29. Laghari, J. R.; Hammoud, A. N. *IEEE Trans. Nucl. Sci.* **1990**, *37*, 1076.
30. Barbir, F. PEM Fuel Cells: Theory and Practice, Elsevier Academic: London, **2005**.
31. Havriliak, S.; Watts, D. G. *Polymer* **1986**, *27*, 1509.
32. Kang, P. H.; Lee, C.; Kim, K. Y. *J. Ind. Eng. Chem.* **2007**, *13*, 250.
33. Shinyama, K.; Fujita, S. *IEEE Trans. Dielect. Elect. Insul.* **2001**, *8*, 538.
34. Fujita, S.; Baba, M.; Shinyama, K.; Suzuki, T. Proceedings of 1995 IEEE 5th International Conference on Conduction and Breakdown in Solid Dielectrics 1995; Leicester, England, USA, IEEE; p 59.
35. Al Lafi, A. G.; Hay, J. N. *J. Polym. Sci. Part B: Polym. Phys.* **2009**, *47*, 775.
36. Huo, P.; Cebe, P. *Macromolecules* **1992**, *25*, 902.
37. Goodwin, A. A.; Simon, G. P. *Macromolecules* **1995**, *28*, 7022.
38. Schönhals, A.; Schlosser, E. *Colloid Polym. Sci.* **1989**, *267*, 125.
39. Schönhals, A.; Kremer, F.; Schlosser, E. *Phys. Rev. Lett.* **1991**, *67*, 999.
40. Andjelić, S.; Fitz, B.; Mijović, J. *Macromolecules* **1997**, *30*, 5239.
41. Böhmer, R.; Ngai, K. L.; Angell, C. A.; Plazek, D. J. *J. Chem. Phys.* **1993**, *99*, 4201.
42. Kunal, K.; Paluch, M.; Roland, C. M.; Puskas, J. E.; Chen, Y.; Sokolov, A. P. *J. Polym. Sci. Part B: Polym. Phys.* **2008**, *46*, 1390.